Icarus 241 (2014) 397–408

Contents lists available at ScienceDirect

Icarus

journal homepage: www.elsevier.com/locate/icarus

Titan's emission processes during eclipse

P. Lavvas [a,*], R.A. West [b], G. Gronoff [c], P. Rannou [a]

[a] GSMA UMR 7331, Universite de Reims, Champagne-Ardene, Reims 51687, France
[b] Jet Propulsion Laboratory, California Inst. of Tech., Pasadena 91109, USA
[c] SSAI/NASA LaRC, Science Directorate, Chemistry and Dynamics Branch, Hampton, VA, 23681-2199, USA

ARTICLE INFO

Article history:
Received 16 March 2014
Revised 25 May 2014
Accepted 3 July 2014
Available online 18 July 2014

Keywords:
Titan
Eclipses
Aurorae

ABSTRACT

Observations of Titan's emissions during its 2009 eclipse by Saturn revealed a weak airglow around the moon, as well as a brighter emission from its disk (West et al. [2012]. Geophys. Res. Lett. 39 (1), 18204). We explore here the potential mechanisms that could generate these emissions and more specifically the role of magnetospheric plasma and cosmic rays in the upper and lower atmosphere, respectively. We consider excitation of N_2 by these energy sources and calculate the resulting emissions through a detailed model of N_2 airglow followed by careful radiation transfer of the emitted photons through the atmosphere, and into the UVIS and ISS instruments. Our results indicate that the observed limb emissions are consistent with magnetospheric plasma energy input, while emissions instigated by cosmic ray excitation are very weak and cannot explain the observed disk emissions. We discuss possible contributions from other sources that could potentially explain the disk observations. The most likely scenario is that of scattered stellar light from Titan's disk.

1. Introduction

Titan's complex atmosphere–surface interaction is dominantly energy driven by the solar radiation, although contributions by secondary energy sources, such as energetic particles from Saturn's magnetosphere and cosmic rays can be important (see Galand et al., 2014, and references therein). Separation though of the solar from the non-solar components is not straight forward; high energy solar photons can penetrate deep in the night-side and contribute to the ionization in the upper atmosphere (Ågren et al., 2009). Given the temporal character of the magnetospheric input, accurate separation of these two components is not straight-forward, therefore observations on Titan's night-side cannot provide a precise description of the non-solar energy sources.

The 2009 spring equinox of the Saturnian system gave us the rare opportunity to observe for the first time Titan in the shadow of Saturn, whence any contribution of solar light is diminished, and a direct evaluation of the contribution of non-solar energy sources can be made. Cassini observations by the Imaging Science Subsystem (ISS) and the UltraViolet Imaging Spectrograph (UVIS) revealed that in the absence of solar radiation the Titan demonstrates a weak but quasi-homogeneous airglow both on the disk and on the limb, with the former being significantly brighter than the latter at visible wavelengths (West et al., 2012; Ajello et al., 2012). These observations constitute a direct evidence for the impact of non-solar energy deposition processes in Titan's atmosphere.

The goal of the current study is to evaluate the potential mechanisms that generate the observed airglow during the eclipse. The fact that the disk is brighter than the limb in the ISS images implies that a source of emission must be located in the lower atmosphere. On the other hand, the observed emissions at UV wavelengths require a source at a relatively optically thin region of the atmosphere in order to survive atmospheric attenuation. Hence there have to be two (at least) mechanisms involved in the generation of the observed emissions. Our approach here is to simulate the anticipated emissions assuming energy deposition by magnetospheric plasma in the upper atmosphere and cosmic rays in the lower atmosphere, and compare these simulations with the available observations.

In order to gain more constraints from the available ISS observations regarding the properties of the emitted radiation we have extended the analysis described in West et al. (2012) with the use of more images. We describe this analysis in Section 2. The simulation of the observations is described in Section 3 and can be separated into three main steps: first we evaluate the production rate of different nitrogen states from the energy deposition of magnetospheric plasma and cosmic rays in Titan's atmosphere, second we calculate the population of these states at different levels of the atmosphere and the associated local emissions from radiative

* Corresponding author.
E-mail address: panayotis.lavvas@univ-reims.fr (P. Lavvas).

http://dx.doi.org/10.1016/j.icarus.2014.07.008
0019-1035/

transitions, and third we perform a detailed radiation transfer calculation of these local emissions through the atmosphere and into the Cassini instruments. We finally discuss potential contributions to the observations from other sources (Section 4).

2. Observations

In this section we discuss the Cassini observations used in our study. From the UVIS instrument we use the observations already presented in West et al. (2012), while for the ISS images we extend the former analysis with the use of multiple filters.

2.1. ISS

The images we use correspond to four different filter combinations for clear, violet, blue and infrared wavelengths taken on May 7, 2009 (Table 1). All images were captured with 560 s exposures, a gain of 12 e^- per Data Number (DN) – the highest gain available – , a lossy compression, and where stored using Lookup Tables (LUT). The latter approximately stores the square root of the observed signal, which although reduces significantly the storage volume required, produces a coarser quantization. Cassini was at an average distance of ~660,000 km during these observations, which for the Wide Angle Camera (WAC) used, corresponds to a pixel size of approximately 40 km. The strongest emissions are observed on the clear filter combination (W1620382876) and we use this image to describe the analysis performed to all images.

First the LUT transformation of the image data to linear DN was performed, followed by a calibrations of the image using the Cassini ISS calibration algorithm (CISSCAL) in order to convert linear DN to physical units of intensity (photons cm^{-2} nm^{-1} s^{-1} sr^{-1}). In short this algorithm corrects the image for bias and dark current, removes the 2-Hz noise, flat-fields, and performs the unit conversion (Porco et al., 2004). The calibrated image needs to be further corrected for point spread function effects (West et al., 2010), which we removed with the application of a maximum likelihood deconvolution algorithm (e.g., Frieden, 1972). Finally, we need to separate the in situ component of the emitted radiation from any contribution of light originating from Saturn's limb and rings, and scattered by Titan to the ISS field of view. This correction was performed by subtracting a scaled imaged of Titan captured during direct sunlight at the same phase angle and filter combination, and scaled at the same body size. The absolute scaling of the dayside image was performed in such a manner that the residual intensity is continuous across the terminator as expected for a nightglow process. The region of interest of the final image is shown in Fig. 1 and demonstrates the bright emission at the main haze layer top (300 km) and the faint emission between 300 and 1000 km.

To get a robust estimate of the very weak signal at the limb we can compare the pixel values of the limb with the values of pixels away from the limb. For this purpose we examined histograms of signal values for two annuli, one for the limb between 300 and 1000 km, and one for an annulus of equal area bounded by 1100 and 1639 km altitude (Fig. 2). We use only the lowest few values of the histograms in order to filter out the higher values produced by star trails and cosmic rays, which are abundant. The total number of pixels (over 8000) in each region provides a measure of statistical significance. The region between 1100 and 1639 km serves as a baseline to evaluate the lowest signal and noise levels in the image. The histograms show that the region between 300 and 1000 km is populated less by zero-level pixels and more by pixels

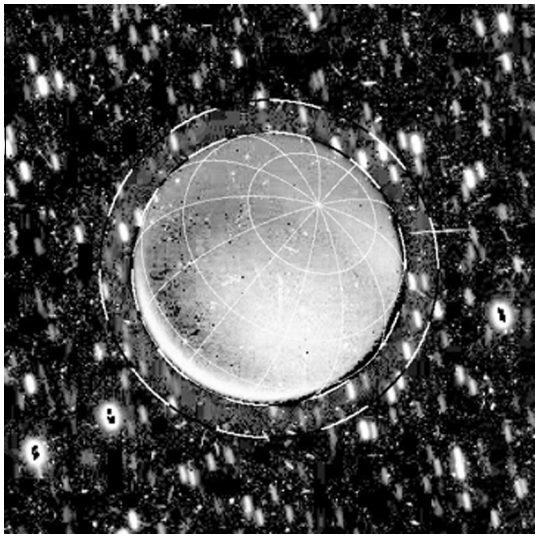

Fig. 1. Portion of a calibrated image of Titan in the [CL1, CL2] filter combination overlaid with a lat./lon. grid. The contribution of scattered light from Saturn has been removed (see text) and the two dashed circles mark the 300 and 1000 km altitude regions that mark the boundaries of the bright disk emission at the top of the main haze layer, and the fainter emission at the limb. Background contributions from star light and cosmic rays are also evident.

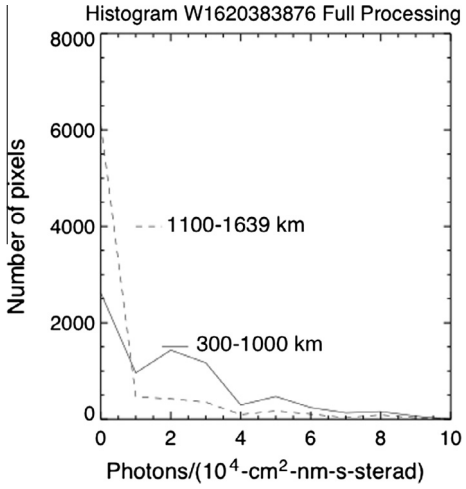

Fig. 2. Histograms of pixel signal values for two annuli bound by 300 and 1000 km, and 1100 and 1639 km altitude for the clear filter calibrated image (Fig. 1). The larger population of pixels with non-zero values for the limb annulus (300–1000 km) is a demonstration of the weak limb emissions with a magnitude of 2–3 × 10^4 photons cm^{-2} nm^{-1} s^{-1} sr^{-1}.

Table 1
List of ISS images analyzed along with the derived DN values.

Image	Image mid time (UTC)	Filters	λ_c (nm)	Distance (km)	⟨Limb DN⟩	⟨Disk DN⟩
W1620379032	2009-127T08:31:22.675	CL1, BL1	460	644030.77	1.1	4.5
W1620381930	2009-127T09:19:40.705	CL1, VIO	420	658002.55	0.2	0.7
W1620383876	2009-127T09:52:06.718	CL1, CL2	635	667326.14	11	71.7
W1620385882	2009-127T10:25:32.731	IR2, CL2	853	676887.08	0.5	6.5